

Investigation of a preamplifier noise in a pulse-echo mode

L. Svilainis, V. Dumbrava

Signal processing department, Kaunas University of technology,

Studentu str. 50, LT-51368 Kaunas, Lithuania, tel. +370 37 300532, E-mail.:svilnis@ktu.lt

Introduction

Recent improvements of noise parameters of operational amplifiers allow their application in low noise ultrasonic preamplifiers. Several papers were published recently discussing these possibilities [1, 2, 3]. Thanks to input circuit simplicity, a noise model, including a simplified ultrasonic transducer model, has been developed [1, 2]. But when it comes to the preamplifier, operating pulse in a echo mode (refer to Fig.1), input circuits become more complex and design of a low noise input stage requires of a new investigation.

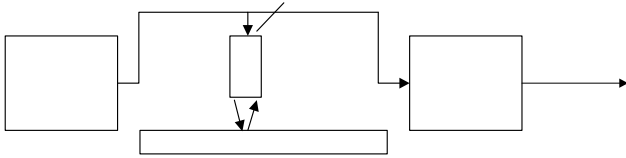


Fig. 1. Pulse – echo ultrasonic system set-up

In this paper we will analyze the noise of the preamplifier, operating in a pulse-echo mode. This type of operation assumes the presence of high energy excitation pulses at the preamplifier input. Therefore the preamplifier should contain a protection circuits. Having analyzed differences introduced by a new circuitry, one can have a map for noise improvement.

Preamplifier noise model for a pulse-echo mode

We shall concentrate on a most common solution for input protection – hard limiter. Such preamplifier circuit diagram is presented in Fig.2.

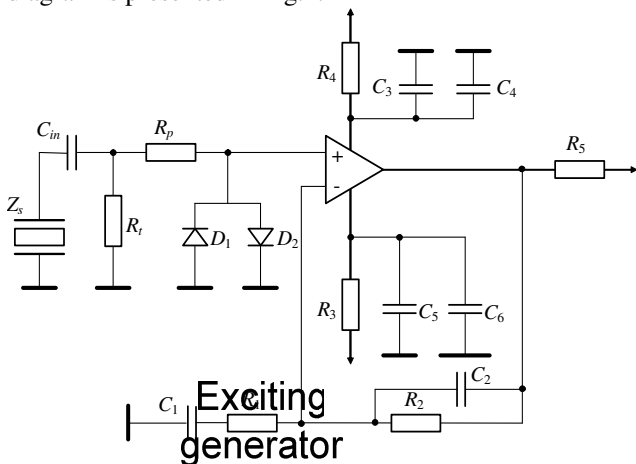


Fig. 2. Preamplifier including input limiter schematics

It contains the ultrasonic transducer Z_s , it's terminating resistor R_t , the alternating current (AC) coupling capacitor

C_{in} , the bipolar limiter, containing R_p and two diodes D_1 , D_2 connected against each other. The operational amplifier is connected in a non-inverting configuration, the gain is set by R_1 and R_2 :

$$G = \frac{R_1 + R_2}{R_1} \quad (1)$$

The capacitor C_2 is added for stability, creating the low-pass cut-off frequency:

$$f_0 = \frac{1}{2\pi R_2 C_2} \quad (2)$$

This value will be used to define the range of integration over frequency. The resistor R_t is used for an input impedance control and control of the operational amplifier bias current. The resistors R_3 , R_4 and capacitors C_3 , C_4 , C_5 , C_6 are used for power supply noise decoupling. The resistor R_5 is used for transmission line impedance matching and current limiting. The capacitor C_1 is used for DC current cancellation in order to reduce amplifier input bias currents mismatch caused by the output direct current (DC) offset.

Using the same approach as in paper [4], we obtain the preamplifier noise equivalent circuit, presented in Fig.3.

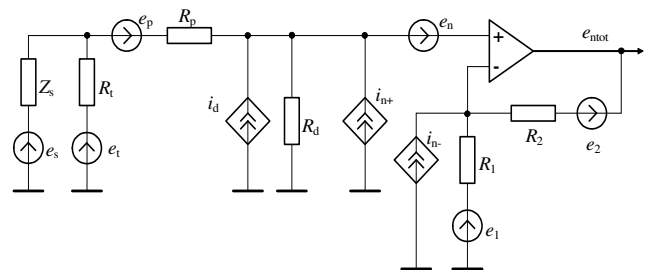


Fig. 3. Preamplifier noise model circuit including input limiter

The new introduction is the limiter diode model. The diode, as a noise generator, is modeled as a current source with an intrinsic resistance inversely proportional to the DC current I_0 flowing through a diode [5]:

$$R_d = \frac{kT}{qI_0} \quad (3)$$

Transducer

where $k=1.380658 \cdot 10^{-23}$ [J/C] is the Boltzmann constant, T is the absolute ambient temperature, $q=1.6 \cdot 10^{-19}$ [C] is the electron charge. The diode noise is dominated by the shot noise so the current spectral density i_d is proportional to the square root of I_0 :

$$i_d = \sqrt{2I_0 q} \quad (4)$$

Analyzing the circuit diagram presented in Fig.2 one can deduce that the only source for I_0 is the operational amplifier bias current. This current is divided between the

Next stages :
filters, TVG,
ADC, DSP

Low noise
preamplifier

Test object

path R_p-R_t and one of diodes (other will be in a reverse bias). Finding the part of the current which flows through the diode is complicated due to the diode's nonlinearity. Taking into account low currents, the diode DC current can be approximated as:

$$I_0 = I_{R0} \left[e^{\frac{U_0}{U_T}} - 1 \right], \quad (5)$$

where U_0 is voltage across the diode, I_{R0} - diode reverse bias current, U_T - temperature potential.

Solving for a static diode resistance and taking into account a parallel connection of R_d and the path R_p-R_t , using operational amplifier bias current for such a resistor, the voltage U_0 is obtained. Then, from Eq. 4 I_0 is obtained. This current then is used in calculation of diode noise parameters.

The parasitic capacitance of a diode will influence the signal bandwidth, so the behavior of diode is modeled by Z_d . The input impedance of operational amplifier must also be taken into account [6]. It is prevailed by a capacitance. Since this capacitance C_{in} is connected in parallel to the limiter diode, for simplification of calculations we put this capacitor together with the diode capacitance, ending:

$$Z_d = R_d + \frac{1}{j\omega(C_d + C_{in})}. \quad (6)$$

Taking all the mentioned above into account, we get the voltage noise spectral density expression for a preamplifier, operating in a pulse – echo mode:

$$\begin{aligned} \frac{e_{ntot}^2}{Hz} = & \left(\frac{R_1 + R_2}{R_1} \right)^2 \times \\ & \times \left[\frac{e_s^2 \cdot R_t^2 + e_t^2 \cdot |Z_s|^2 + e_p^2 \cdot |Z_s + R_t|^2}{|R_p + Z_d|^2 \cdot |R_t + Z_s|^2} \times |Z_d^2| + (i_{n+}^2 + i_d^2) \times |Z_{STP}|^2 \right] + \\ & + \left(\frac{R_1 + R_2}{R_1} \right)^2 \cdot e_n^2 + \left(\frac{R_2}{R_1} \right)^2 \cdot e_1^2 + e_2^2 + R_2^2 \cdot i_{n-}^2 \end{aligned} \quad (7)$$

where

$$Z_{STP} = \frac{\left[\frac{Z_s \cdot R_t}{Z_s + R_t} + R_p \right] \cdot Z_d}{\frac{Z_s \cdot R_t}{Z_s + R_t} + R_p + Z_d}. \quad (8)$$

The noise RMS value at the amplifier output can be calculated as:

$$E_{esRMS} = \sqrt{\int_{f_1}^{f_2} e_{ntot}^2 df}, \quad (9)$$

where f_1 and f_2 are the lower and upper boundaries for integration. As already mentioned above, the frequency f_1 is defined by C_1 value, and the frequency f_2 by C_2 .

Noise analysis

Using the equations obtained, the output voltage noise RMS of the preamplifier dedicated for a pulse – echo mode was investigated theoretically. The operational amplifier and the transducer considered as an optimal pair in [2] were used. Having no ability to use the same transducer as

used in the source, the transducer with close parameters was used. Both transducers parameters are presented in Table 1.

The results are presented in Fig.4. The diode was not included at this stage of investigation. In order to have an experimental verification, the circuit in Fig. 2 was assembled without the diodes. Then, the values were measured using a RMS voltmeter. These values are presented by the dark large dots in Fig.4. Note the level of e_n contribution to the output noise, indicated by dashed line.

Table 1. Transducer parameters

Transducer	R_s, Ω	C_s, pF	L_s, uH	C_o, pF
Source [2]	1800	26	1600	65
Alternative	430	92	1060	250

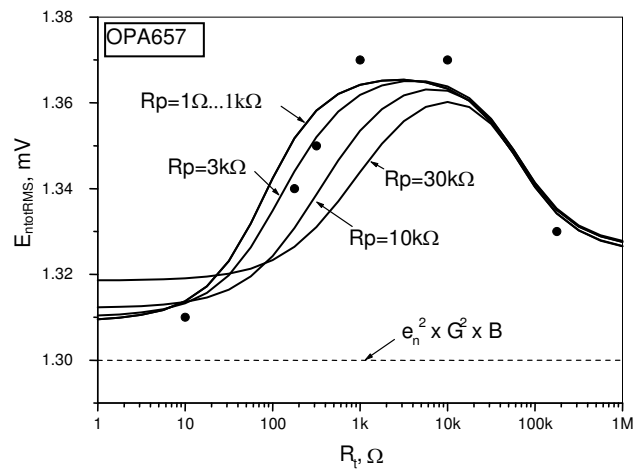


Fig. 4. Output noise RMS using model and experiment (dots)

Both investigations revealed an interesting phenomenon – adding the limiter resistor and increasing its value, the noise RMS is decreasing. This is because the input parasitic capacitance of the operational amplifier is creating a RC low-pass filter, so it is limiting the noise portion coming into the amplifier. In Fig.5 we have plotted output noise power spectral density for same values of R_p as in Fig.4. The resistor R_t is 1 kΩ.

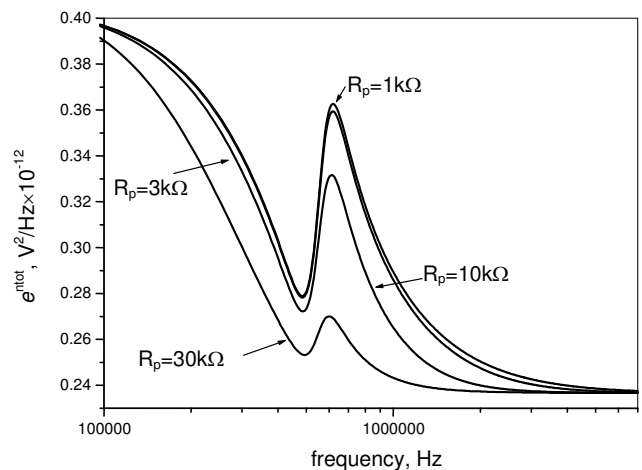


Fig. 5. Output noise power density

It can be seen that noise spectra is bandwidth limited with increase of R_p . Even at the value of 10 k Ω the bandwidth is getting narrower than the transducer resonant frequency. Therefore either use of R_p values above 3 k Ω should be avoided or R_p should be accompanied by a parallel frequency compensation capacitor in order to have a sufficient bandwidth for passing of the signal.

The next stage of investigation concentrated on diode noise. The R_p was chosen 1 k Ω . Again, both model calculations and experiment were carried out. The results are presented in Fig.6.

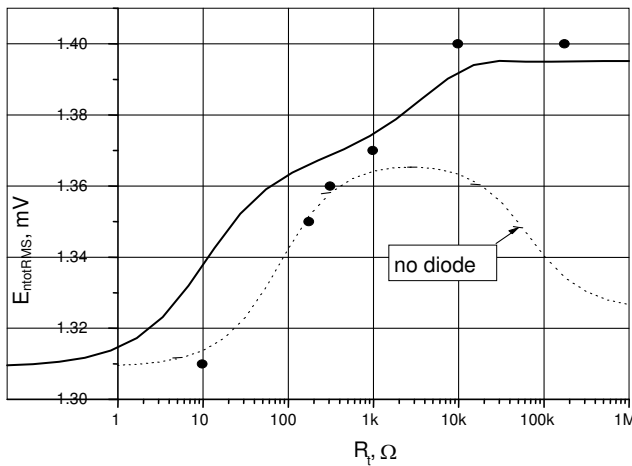


Fig.6. Preamplifier output noise RMS using model and experiment (dots) with a diode included

The experimental and modelling results show that application of a diode is increasing the total output noise at high terminating resistor values. We think that this rise in a noise is due to the diode bias current increase at a high resistance, connected in parallel to the diode (R_p - R_t path). For this purpose we have investigated the diode contributed output noise part. The results of noise change with the terminating resistor R_t investigation are presented in Fig.7.

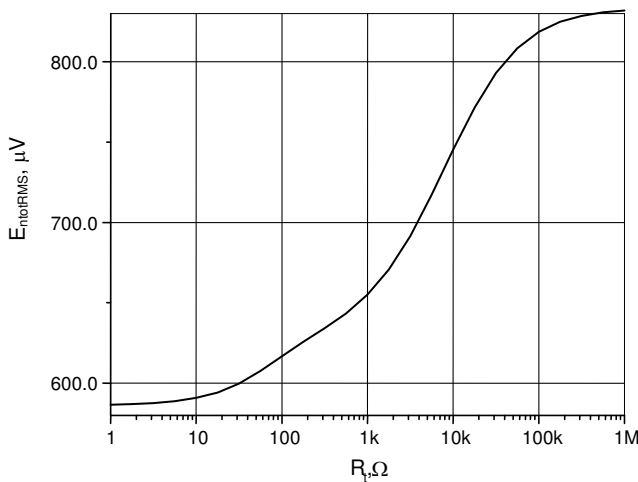


Fig. 7. Diode contributed output noise

It is evident from the graph presented that the diode noise is contributed only at high values of the resistor R_t .

Therefore one might expect the reduction of a diode noise if the diode current cancellation scheme is applied [6, 7].

In order to obtain the recommendations for R_p value, we have investigated two operational amplifiers, representing two opposite choices by means of e_n to i_n ratio. Refer to Table 2 for the parameters of amplifiers.

Table 2. Amplifier noise parameters

Amplifier	$e_n, \text{nV}/\sqrt{\text{Hz}}$	$i_n, \text{fA}/\sqrt{\text{Hz}}$
LMH6624	0.95	2300
OPA657	4.8	1.3

The results of R_p influence at the termination resistor R_t chosen $100 \times R_s$ are presented in Fig.8 and Fig.9.

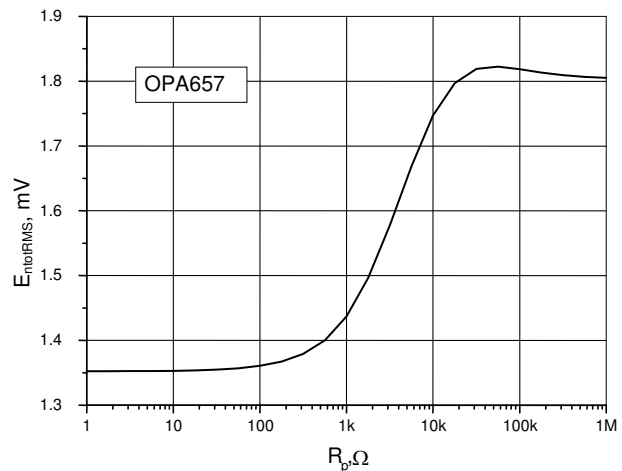


Fig. 8. Output noise versus limiter resistor R_p for OPA657

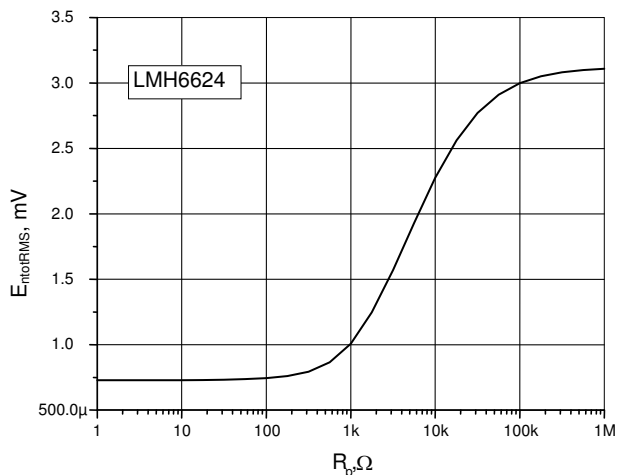


Fig. 9. Output noise versus limiter resistor R_p for LMH6624

From the graphs presented above it can be seen that in both cases, independently on the type of an amplifier, the optimal R_p value is below 1 k Ω .

Conclusions

As it can be seen from the analysis above limiting circuits degrade the output noise of an amplifier.

Readers should be beware, that recommendations are given for circuit values for a particular transducer. In order

to have optimal circuit values for other transducer type, the analysis should be repeated again using the same approach as in this paper.

Acknowledgements

We would like to thank Giedrius Motiejūnas for his help in circuit assembly.

References

1. **Dumbrava V., Svilainis L.** Design of low noise preamplifier for ultrasonic transducer. *Ultragarsas*. Kaunas: Technologija. 2005. No.2(55). P.28-32.
2. **Yanez Y., Garcia – Hernandez M. J., Salazar J., Turo A., Chavez J. A.** Designing amplifiers with very low output noise for high impedance piezoelectric transducers. *NDT&E International* 2005. Vol.38. P. 491-496.
3. **Turo A., Salazar J., Chavez J. A., Kichou H. B., Gomez T. E., Montero de Espinoza F., Garcia – Hernandez M. J.** Ultra-low noise front–end electronics for air–coupled ultrasonic non-destructive evaluation. *NDT&E International* 2003. Vol.36. P. 93-100.
4. **Dumbrava V., Svilainis L.** Noise model for ultrasonics transducer preamplifier. *Elektronika ir elektrotechnika*. Kaunas: Technologija. Submitted for publication.

5. **H Ott.** Noise reduction techniques in electronic systems. 2nd Edition Wiley-Interscience. 1988.
6. **Motchenbacher C. D., Connelly J. A.** Low-noise electronic system Design Wiley-Interscience. 1993.
7. **David A. J., Ken M.** Analog integrated circuit design. New York: John Wiley & Sons. 1997.

L. Svilainis, V. Dumbrava

Siuntimo ir priėmimo režimu dirbančio pradinio stiprintuvo triukšmų tyrimas

Reziumė

Nagrinėjami pradinio stiprintuvo, skirto dirbti siuntimo ir priėmimo režimu, triukšmai. Dėl šio režimo specifikos stiprintuvo įėjimo grandinės papildomos ribotuvu, skirtu apsaugai nuo aukštos įtampos žadinančių impulsų. Sudarius visą elektroakustinio trakto triukšminį modelį, atlikta ribotuvo grandinių įnešamų triukšmų analizė. Parodyta, kad šios grandinės blogina triukšmines pradinio stiprintuvo charakteristikas ir triukšmų požiūriu yra nepageidautinos. Atlikti eksperimentiniai tyrimai. Pateikiamos rekomendacijos dėl šių grandinių optimizavimo siekiant maksimalaus signalo ir triukšmo santykio.

Pateikta spaudai 2005-09-26